ELSEVIER

Soil alteration by continued oxidation of pyrite tailings

F. Martín [a,*], I. García [b], M. Díez [a], M. Sierra [a], M. Simon [b], C. Dorronsoro [a]

[a] *Departamento Edafología y Química Agrícola, Faculty of Sciences, University of Granada, Campus Fuentenueva s/n, 18002 Granada, Spain*
[b] *Departamento Edafología y Química Agrícola, CITE IIB, University of Almería, Carretera Sacramento s/n, 04120 Almería, Spain*

Abstract

This work examines the alteration processes triggered after the oxidation of pyrite tailings deposited for 3 years over a carbonate soil. The infiltration of the acidic solution into the soil is causing important morphological, compositional and mineralogical changes in the profile. After 3 years of continued action of such alteration, a considerable degradation of the main soil properties was evident, the most notable being the decline in the cation-exchange capacity (caused by the decreases in clay and organic matter content), texture variation, greater electrical conductivity (10-fold greater than in unaffected soil), and the appearance of horizons with colorations strongly differing from those of the original soil (a discoloured layer with greyish tonalities in the first 5 mm, followed by a reddish-brown layer to a depth of 65–70 mm). At the same time, the carbonates have weathered, disappearing completely from the upper 35 mm and partially to 80 mm in depth. There has also been an intense acidification of the soil (with pH values close to 2.0 within the greyish layer) as well as a partial hydrolysis of the primary silicates (mainly feldspars and phyllosilicates), causing extreme infertility of the soil. The resulting products in this process give rise to intense neoformation of gypsum and hydroxysulphates of Fe and Al, which, together with the acidic conditions of the medium, determine the distribution of the main elements of the soil, both in their total and soluble forms.

© 2008 Elsevier Ltd. All rights reserved.

1. Introduction

The oxidation of sulphides, a complex biogeochemical process (Nordstrom, 1982) involving hydration, oxidation, and hydrolysis, can be summarized in a simplified form in the reaction proposed by Stumm and Morgan (1981)

$$FeS_2 + 3.75O_2 + 3.5H_2O \rightarrow Fe(OH)_3 + 2H_2SO_4$$

This generalised reaction involves a sequence of reactions beginning with the release of Fe^{2+}, which under oxidizing conditions is converted into Fe^{3+}. If the pH of the medium remains above 4.5 (e.g. in carbonate media), this Fe(III) precipitates as a hydroxide, generating more acidity in the medium:

$$Fe^{3+} + 3H_2O \rightarrow Fe(OH)_3 + 3H^+$$

The final result of the oxidation of pyrite under these conditions strongly acidifies the medium (for each mole of pyrite oxidized 4 mol of H^+ are produced). If, on the contrary, the pH of the medium stays under 4.5, the Fe^{3+} can act as an oxidant of the pyrite

---

* Corresponding author. Tel.: +34 958 243233; fax: +34 958 244160.
E-mail address: fjmartin@ugr.es (F. Martín).

$$FeS_2 + 14Fe^{3+} + 8H_2O \rightarrow 15Fe^{2+} + 2SO_4^{2-} + 16H^+$$
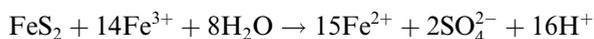
At pH < 3.0 the Fe^{3+} is considered the only oxidizing agent of these sulphides (Nordstrom, 1982). This latter oxidation is far faster than reactions that operate when the pH is higher (pH > 3.0) and generates much greater acidity. Furthermore, these reactions accelerate enormously in the presence of certain bacteria (*Thiobacillus ferrooxidans, Leptospirillum ferrooxidans* and *Thiobacillus thiooxidans*) and can increase normal oxidation rates by 10^5 or 10^6 (Lacey and Lawson, 1979; Bigham and Nordstrom, 2000).

The other product generated during pyrite oxidation is SO_4^{2-}. Under the acidic conditions induced by pyrite oxidation, the elements usually accompanying pyrite are highly mobile and most SO_4^{2-} complexes that may form are highly soluble and remain potential pollutants.

The acidifying tendency of these types of reactions is heavily influenced by the neutralization capacity of the surrounding medium. In the case of a soil, this capacity is closely related to its properties and mineralogical composition. According to Palmer (1978), the main buffering reactions that act in the soil with a fall in pH are: cation exchange, the alteration of silicates, the dissolution of Fe and Al hydroxides, and the dissolution of carbonates. Of these reactions, the dissolution of carbonates is the most effective, resulting in according to the simplified scheme of Williams et al. (1982)

$$FeS_2 + CaCO_3 + 15/4O_2 + 3/2H_2O$$
$$\rightarrow Fe(OH)_3 + 2SO_4^{2-} + 2Ca^{2+} + 2CO_2$$
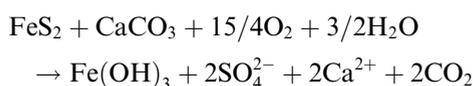
where the acidity is neutralized by the reaction between the carbonates and the products released in the oxidation process (Ritsema and Groenenberg, 1993)

$$CaCO_3 + 2H^+ + SO_4^{2-} + H_2O$$
$$\rightarrow CaSO_4 \cdot 2H_2O + CO_2$$
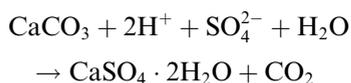
Therefore, the formation of gypsum, very common in these media, is related to three origins: dissolution of Ca carbonates, hydrolysis of minerals containing Ca, and desorption of exchangeable Ca (Van Breemen, 1973). Thus, in addition to neutralising acidity and maintaining pH conditions above 4.0, the presence of reactive $CaCO_3$ inhibits pyrite oxidation by inactivating *T. Feroxidans* and

promoting the precipitation of Fe^{3+} (as ferric oxyhydroxides) that could otherwise act as an oxidant and accelerate pyrite decomposition.

In 1998 the holding pond for the tailings of a pyrite mine in Aznalcóllar (Seville, SW Spain) failed and spilled some $4.5 \times 10^6 \, m^3$ of tailings and acidic waters with a high concentration in S, Fe and potentially harmful elements into the Agrio and Guadiamar rivers, affecting some $45 \, km^2$ of fertile land (Simón et al., 1999; López-Pamo et al., 1999). In the tailings the pyrite content was between 85 and 90% (Alastuey et al., 1999) while the main pollutants were Zn, Pb, Cu, As and Cd. The subsequent drying and aeration of the tailings deposited over the soil resulted in an intense and rapid oxidation of the sulphides that heavily affected the soils involved, raising previous contaminant levels by 4.5-fold in these soils (Simón et al., 2001).

The present work examines the alteration processes triggered after the oxidation of pyrite tailings deposited for 3 years over a carbonate soil in experimental plots in the affected area, paying special attention to the effect of the acidic solution on the soil properties and constituents, the mobility of the major elements involved, and the mineralogical transformations taking place in the affected soil.

2. Materials and methods

In the zone of Aznalcóllar affected by the spill of pyrite tailings, two plots have been preserved (in the area known as Vado del Quema) without any remediation and maintaining the layer of tailings that covered the soil surface after the accident (Dorronsoro et al., 2002; Simón et al., 2002).

The soil studied was a calcareous Regosol (FAO-ISRIC-ISSS, 1998) with scant development, a sandy-loam texture (12% clay), little organic matter ($< 2\%$), a mean $CaCO_3$ content equivalent of 13%, and a pH close to 8.0.

The first sampling (Q0) was made at 40 days after the spill and the second (Q1) 3 years later. At the time of sampling, the Q0 soil was covered by a 4.5 cm thick layer of tailings having a brownish colour (2.5Y5/4) that was homogeneous in depth. The soil Q1 (still covered by the tailings) presented a strong morphological difference. Immediately underneath the tailings appeared a layer light grey in colour (2.5Y7/2) averaging 5 mm in thickness, followed by a reddish-brown (10YR5/6) layer 70 mm thick, and finally the underlying soil,

apparently unaltered, brown in colour (2.5Y5/4), and very similar to the soil Q0 (Fig. 1).

Systematic sampling was performed in the two periods to examine textural, mineralogical, and compositional trends as a function of depth. A hole 1×2 m and 0.8 m depth was dug and 3 of its walls were sampled in triplicate. In the Q0 soil, a sample was taken every 5 mm to a depth of 20 mm, then every 20 mm to a depth of 100 mm, and finally every 50 mm to a depth of 550 mm. In Q1, a sample was taken every 5 mm to a depth of 70 mm, then every 10 mm to a depth of 120 mm, and finally every 50 mm to a depth of 570 mm.

The samples were air dried and then screened to 2 mm to determine the percentage of gravel and fine earth, all the analyses being made over the latter fraction. The particle-size distribution was analysed by the pipette method (Loveland and Whalley, 1991) for the fraction finer than 50 μm (silt and clay), and by sieving for the fraction between 50 μm and 2 mm (sand). This textural analysis was also made after treatment with a dithionite–citrate–bicarbonate (DCB) solution to eliminate the Fe oxides (Sheldrick and Wang, 1993). The pH of the samples was determined potentiometrically in a 1:2.5 suspension, and the content of $CaCO_3$ equivalent was measured by the method of Williams (1948). The cation-exchange capacity (CEC) was determined with 1 N sodium acetate at pH 8.2. The total concentrations of major elements (Si_T, Al_T, Fe_T, Ca_T, Mg_T, Na_T, K_T, S_T) were determined after preparing soil pellets with lithium tetraborate 0.6:5.5, by X-ray fluorescence in a Philips PW-1404 apparatus.

Finally, soil extracts were prepared at a soil:water ratio of 1:10 (Norma DIN, 38 414-4) to measure: the pH, electrical conductivity (EC) and the concentrations of the soluble fractions of major components; Na_S and K_S were determined by flame photometry (METEOR NAK-II instrument), Ca_S, Mg_S, Fe_S and Al_S by atomic absorption spectrometry (VARIAN SpectrAA 220FS instrument), and soluble SO_4^{2-} by ion chromatography (DIONEX DX-120 instrument).

For the micromorphological study and the analysis of the mineral composition, a microscope with polarized light and a LEO-1530 GEMINI scanning electron microscope were used, the latter with a Link Pentafet energy-dispersive X-ray microanalyser (EDX), Oxford model 6901. The mineralogy was also studied by X-ray diffraction with a Philips PW-1710 with CuKα radiation, Ni-filter and graphite monochromator, using the method of disoriented crystalline powder.

3. Results

3.1. Soil properties and constituents

The main properties and constituents of the soil before and after the oxidation of the tailings (Q0 and Q1, respectively) are shown in Tables 1 and 2. The comparison of soil properties and constituents in the samples of soil Q1 deeper than 200 mm, with the soil Q0, indicated no significant differences between them, and the variations may be due to the heterogeneity of the soils. The property that had undergone the most notable changes during the study period was acidity, reflected in the substantial fall in pH as the contamination progressed. The Q0 soil gave a mean value of 7.9, while Q1 reached pH values close to 2.0 in the samples closest to the tailings; values lower than 4.0 in the first 30 mm, and significant effects to a depth of
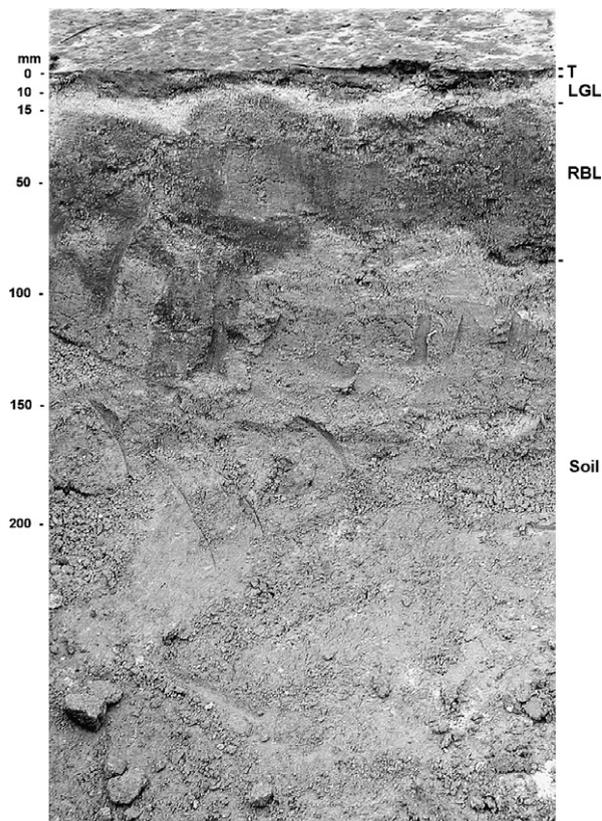
Fig. 1. General view of soil Q1 (T: tailings; LGL: light-grey layer; RBL: reddish-brown layer).

Table 1
Main properties of soil before the oxidation of tailing (Q0)

Depth (mm)	pH		CaCO$_3$ (%)		CEC (cmol$_+$ kg^{-1})		OM (%)		EC (dS m^{-1})		Clay (%)		F. Silt (%)		C. Silt (%)		Sand (%)	
	Mean	SD	Mean	SD	Mean	SD	Mean	SD	Mean	SD	Mean	SD	Mean	SD	Mean	SD	Mean	SD
0–5	7.63	0.08	8.12	1.02	29.19	1.22	2.29	0.20	0.92	0.12	29.5	1.4	30.3	1.7	21.3	1.9	18.9	1.6
5–10	7.91	0.05	8.61	1.15	32.65	1.54	2.27	0.39	0.85	0.16	33.3	1.9	38.1	2.1	10.2	2.5	18.4	1.9
10–15	7.92	0.08	9.04	0.77	25.74	2.81	2.15	0.07	0.57	0.07	32.7	2.9	34.9	2.8	11.2	2.9	21.2	2.3
15–20	7.82	0.08	9.23	0.92	29.29	1.06	2.12	0.14	0.52	0.18	35.5	1.2	36.1	1.6	16.6	1.7	11.8	1.4
20–40	7.93	0.06	8.97	0.52	17.19	1.50	1.78	0.68	0.42	0.12	32.2	2.2	31.2	2.3	18.3	2.0	18.3	2.2
40–60	7.98	0.03	9.15	0.65	17.19	1.37	1.78	0.72	0.45	0.07	32.0	2.1	30.6	2.1	16.5	2.9	20.9	2.1
60–80	8.10	0.08	8.87	0.82	12.87	2.14	1.75	0.52	0.42	0.10	33.2	2.7	29.1	2.8	14.6	2.3	23.1	2.7
80–100	8.00	0.06	9.02	0.69	11.14	1.67	1.75	0.58	0.39	0.11	31.1	2.2	31.0	2.4	12.8	2.9	25.1	2.2
100–150	7.90	0.07	9.30	1.22	9.41	2.56	1.68	0.34	0.42	0.08	31.2	2.9	29.1	3.0	12.0	2.3	27.7	2.3
150–200	7.90	0.07	8.91	0.46	8.55	1.30	1.68	0.44	0.36	0.02	28.6	1.7	28.9	2.1	16.2	2.5	26.3	2.1
200–250	7.80	0.07	9.44	0.51	10.19	1.57	1.59	0.06	0.41	0.05	32.2	1.6	31.6	2.7	11.7	2.7	24.5	2.6
250–300	7.90	0.09	9.10	0.74	12.87	1.35	1.59	0.31	0.34	0.03	39.9	1.7	28.5	1.9	13.2	2.2	18.4	1.9
300–350	8.00	0.05	9.33	0.48	9.98	1.61	1.43	0.13	0.38	0.05	33.6	1.7	30.2	1.8	12.8	1.9	23.4	1.7
350–400	7.90	0.07	9.46	0.62	10.20	1.50	1.52	0.38	0.32	0.04	29.8	1.9	28.2	2.1	14.7	2.5	27.3	2.1
400–450	7.80	0.07	9.12	1.14	10.39	2.32	1.49	0.18	0.35	0.06	35.3	2.5	32.4	2.6	11.9	2.7	20.4	2.2
450–500	7.90	0.07	9.34	0.63	9.94	1.66	1.47	0.23	0.33	0.08	31.7	1.9	29.6	2.0	13.9	2.2	24.8	1.9
500–550	7.90	0.06	9.20	0.51	10.10	1.45	1.44	0.24	0.31	0.07	30.2	1.7	31.1	1.8	12.4	2.0	26.3	1.7

SD: standard deviation; CEC: cation-exchange capacity; OM: organic matter; EC: electric conductivity; F. Silt: fine silt; C. Silt: coarse silt.

Table 2
Main properties of soil after the oxidation of tailing (Q1)

Depth (mm)	pH Mean	SD	CaCO$_3$ (%) Mean	SD	CEC (cmol$_+$ kg^{-1}) Mean	SD	OM (%) Mean	SD	EC (dS m^{-1}) Mean	SD	Texture (Na-poliph.) Clay (%) Mean	SD	F. Silt (%) Mean	SD	C. Silt (%) Mean	SD	Sand (%) Mean	SD	Texture (DCB) Clay (%) Mean	SD	F. Silt (%) Mean	SD	C. Silt (%) Mean	SD	Sand (%) Mean	SD
0–5	*2.09*	0.03	*0.00*	0.00	*8.94*	0.82	*1.05*	0.08	*2.70*	0.17	*30.2*	0.9	*22.9*	2.0	*14.0*	1.9	*32.9*	2.1	*31.7*	2.0	*14.6*	1.0	*15.1*	1.0	*38.6*	2.2
5–10	**2.29**	0.05	**0.00**	0.00	**11.69**	0.79	**1.10**	0.12	**2.51**	0.37	**16.9**	0.9	**11.4**	1.2	**11.2**	1.8	**60.5**	1.3	**33.4**	2.2	**14.7**	1.1	**12.1**	1.0	**39.9**	2.5
10–15	**2.38**	0.06	**0.00**	0.00	**10.48**	0.91	**1.05**	0.10	**2.74**	0.31	**14.2**	1.0	**9.6**	1.3	**11.9**	1.0	**64.3**	1.4	**31.0**	1.3	**14.4**	1.2	**16.1**	1.1	**38.5**	1.6
15–20	**2.76**	0.04	**0.00**	0.00	**12.89**	0.86	**1.03**	0.09	**2.10**	0.27	**13.5**	1.0	**7.5**	1.2	**12.4**	0.9	**66.5**	1.3	**31.4**	1.8	**14.4**	1.7	**17.4**	1.0	**36.8**	2.1
20–25	**2.89**	0.05	**0.00**	0.00	**11.70**	1.14	**1.08**	0.07	**1.94**	0.08	**14.4**	1.2	**12.3**	1.2	**6.7**	1.2	**66.5**	1.3	**31.9**	1.2	**15.7**	1.7	**14.7**	1.3	**37.8**	1.3
25–30	**3.21**	0.06	**0.00**	0.00	**14.01**	1.29	**0.96**	0.11	**1.96**	0.18	**14.8**	1.4	**11.1**	1.5	**10.3**	1.3	**63.8**	1.6	**30.3**	1.5	**13.3**	1.4	**17.9**	1.5	**38.5**	1.7
30–35	**4.46**	0.03	**0.00**	0.00	**12.30**	1.03	**1.08**	0.09	**1.87**	0.34	**14.3**	1.1	**10.7**	1.4	**11.2**	1.1	**63.8**	1.5	**30.5**	1.4	**15.1**	1.3	**16.2**	1.2	**38.2**	1.8
35–40	**5.00**	0.05	**1.28**	0.12	**10.50**	0.99	**0.91**	0.08	**1.66**	0.21	**15.2**	1.1	**12.4**	1.2	**10.2**	1.0	**62.2**	1.3	**29.9**	1.2	**14.7**	1.5	**15.5**	1.1	**39.9**	1.4
40–45	**5.29**	0.05	**1.55**	0.16	**12.89**	1.24	**1.10**	0.09	**1.84**	0.15	**12.9**	1.3	**12.4**	1.4	**11.4**	1.2	**63.3**	1.5	**28.7**	1.4	**15.6**	1.3	**14.0**	1.4	**41.7**	2.5
45–50	**5.53**	0.06	**1.46**	0.20	**12.30**	1.34	**1.13**	0.10	**1.89**	0.24	**15.9**	1.4	**12.8**	1.6	**11.5**	1.4	**59.7**	1.7	**28.1**	1.6	**18.0**	1.5	**11.5**	1.5	**42.3**	1.9
50–55	**6.10**	0.08	**1.48**	0.14	**12.89**	1.06	**1.27**	0.07	**1.88**	0.29	**15.4**	1.1	**13.4**	1.3	**10.5**	1.1	**60.6**	1.4	**27.1**	1.3	**17.9**	1.7	**15.7**	1.2	**39.3**	2.6
55–60	**6.27**	0.08	**1.89**	0.10	**12.30**	1.21	**1.30**	0.09	**1.67**	0.12	**15.9**	1.3	**12.5**	1.3	**12.3**	1.2	**59.3**	1.4	**26.8**	1.7	**16.7**	1.6	**17.0**	1.4	**39.5**	1.9
60–65	**6.50**	0.06	**2.91**	0.19	**11.70**	0.89	**1.35**	0.12	**1.60**	0.17	**18.9**	1.0	**13.9**	1.1	**15.2**	1.0	**52.0**	1.2	**26.0**	1.1	**16.2**	1.9	**18.1**	1.1	**39.6**	1.3
65–70	**6.89**	0.08	**3.24**	0.24	**13.50**	1.23	**1.38**	0.08	**1.53**	0.15	**18.5**	1.3	**16.4**	1.4	**12.4**	1.2	**52.7**	1.5	**25.5**	1.4	**17.7**	1.3	**17.0**	1.4	**39.8**	2.5
70–80	7.09	0.05	4.14	0.36	10.09	1.50	1.35	0.05	1.13	0.11	19.9	1.5	17.5	1.5	16.3	1.4	46.3	1.6	24.0	1.5	18.0	1.4	17.8	1.6	40.2	1.6
80–90	7.42	0.07	7.62	0.62	10.09	0.96	1.23	0.06	0.33	0.04	22.8	1.0	20.4	1.6	13.2	1.6	43.6	1.7	25.6	1.6	19.7	1.6	16.6	1.1	38.0	1.7
90–100	7.60	0.07	7.95	0.74	10.70	0.76	1.19	0.06	0.23	0.07	28.4	0.8	20.9	1.2	9.7	0.9	41.1	1.3	27.8	0.9	18.2	1.2	15.9	0.9	38.1	1.8
100–110	7.76	0.06	8.62	0.63	14.10	1.04	1.24	0.08	0.22	0.05	26.0	1.1	14.7	0.9	19.9	1.1	39.3	1.0	25.3	1.1	17.9	1.0	17.3	1.2	39.5	2.2
110–120	7.68	0.07	8.64	1.15	15.91	1.25	1.23	0.05	0.26	0.02	25.7	1.3	21.5	1.3	12.7	1.2	40.1	1.3	26.9	1.5	18.9	1.5	17.1	1.3	37.1	1.5
120–170	7.80	0.07	9.00	0.69	12.34	1.19	1.28	0.07	0.24	0.02	26.1	1.2	20.6	1.0	11.9	1.2	41.5	1.2	28.1	1.1	18.2	0.9	16.2	1.2	37.5	1.6
170–220	7.86	0.09	8.87	0.84	10.08	1.09	1.21	0.05	0.23	0.05	23.2	1.1	21.5	1.6	15.2	1.5	40.0	1.6	24.5	1.6	19.1	1.5	15.8	1.2	40.6	2.6
220–270	7.84	0.05	8.56	0.65	10.08	0.91	1.17	0.06	0.22	0.05	24.8	1.0	17.0	1.3	17.9	1.2	40.3	1.3	25.2	1.8	17.8	1.7	16.6	1.0	40.4	1.9
270–320	8.00	0.08	8.80	0.73	11.58	0.86	1.20	0.05	0.21	0.01	26.6	0.9	17.4	1.1	18.6	0.8	37.3	1.2	27.6	1.4	18.4	1.3	16.1	1.0	37.9	1.4
320–370	7.92	0.08	8.69	0.85	12.35	1.14	1.13	0.07	0.20	0.07	24.6	1.2	20.5	1.2	18.8	1.1	36.0	1.3	28.2	1.2	18.8	1.1	17.5	1.3	35.5	2.3
370–420	7.80	0.06	9.10	1.07	13.22	1.29	1.19	0.04	0.19	0.05	23.7	1.3	19.5	1.4	15.0	1.5	41.9	1.3	26.6	1.5	17.2	1.4	16.9	1.4	39.3	1.6
420–470	7.99	0.05	8.80	0.76	14.50	1.03	1.18	0.05	0.17	0.04	12.8	1.1	9.9	1.3	19.4	1.3	57.9	1.4	24.9	1.4	17.7	1.4	16.2	1.1	41.2	2.5
470–520	7.90	0.08	8.90	0.95	10.57	0.99	1.22	0.06	0.20	0.03	15.1	1.0	9.6	1.3	17.3	1.0	58.0	1.2	25.8	1.0	16.7	0.9	15.9	1.1	41.6	2.0
520–570	8.10	0.07	8.70	0.89	10.69	1.23	1.19	0.05	0.22	0.04	16.6	1.3	13.2	1.2	17.8	1.2	52.5	1.3	28.3	1.5	17.1	1.4	16.3	1.3	38.3	1.8

Italics: light-grey layer; bold: reddish-brown layer. Na-polyph.: soil dispersed with sodium-polyphosphate; DCB: soil treated with dithionite–citrate–bicarbonate; SD: standard deviation; CEC: cation-exchange capacity; OM: organic matter; EC: electric conductivity; F. Silt: fine silt; C. Silt: coarse silt.

100 mm. The EC of the soil solution had an inverse relationship with pH, and the highest values were registered in the first 5 mm of the Q1 soil.

The cation-exchange capacity measurably declined; thus, in the upper part of the Q0 soil, mean values were 30 $cmol_+$ kg^{-1}, while in the same zone the soil values after 3 years (Q1) dropped to 12 $cmol_+$ kg^{-1}. The depth at which CEC was considerably affected coincided with the lower limit of the reddish-brown alteration layer (70 mm) in the soil profile.

The main soil constituents were also affected by the acidic solution, provoking stronger differences in the first 5 mm in relation to the underlying soil, mainly in $CaCO_3$ content and OM (Tables 1 and 2); these differences diminished with depth in the reddish layer, and disappeared in the unaffected soil.

The carbonate mineral of this soil, identified by X-ray diffraction, is calcite, having a dominant grain size coarser than 2 μm (silt and sand); and the mean content of this mineral is about 9% both in the initial soil (Q0) as in the unaffected part of the Q1 soil (depth > 200 mm). The alteration of the calcite is complete in the uppermost 35 mm of the soil affected by the pyrite oxidation (Q1) and partial between 35 and 80 mm (Table 2).

The total concentrations in the main elements (Si_T, Al_T, Mg_T, K_T, Na_T) clearly declined in the upper 70 mm of the Q1 soil and tended to increase with depth (Fig. 2); in addition, the Fe dissolved in the acidic solution tended to precipitate in the upper part of the soil, especially in the first 30 mm, where the total Fe content (Fe_T) was more than double that of the unaffected soil (>200 mm).

The concentration of most of the main elements in the soil solution (Al_S, Fe_S, Mg_S, K_S, Na_S) indicated a generalized increase in the upper part of the soil, due to the intense mineral alteration (Fig. 3), with the exception of soluble K which decreased markedly in the first 50 mm.

3.2. Mineralogical composition

The mineralogy of the Q0 soil was dominated by quartz (60%), calcite (11%), phyllosilicates (15%) and feldspars (14%). The infiltration of the acidic solution from the oxidation of the tailings provoked intense alteration of the primary minerals as well as notable neoformation processes, as reflected clearly in the uppermost mm of soil Q1 (Fig. 4). Thus, intense alteration of calcite was evident, this mineral disappearing completely in the upper zone of the
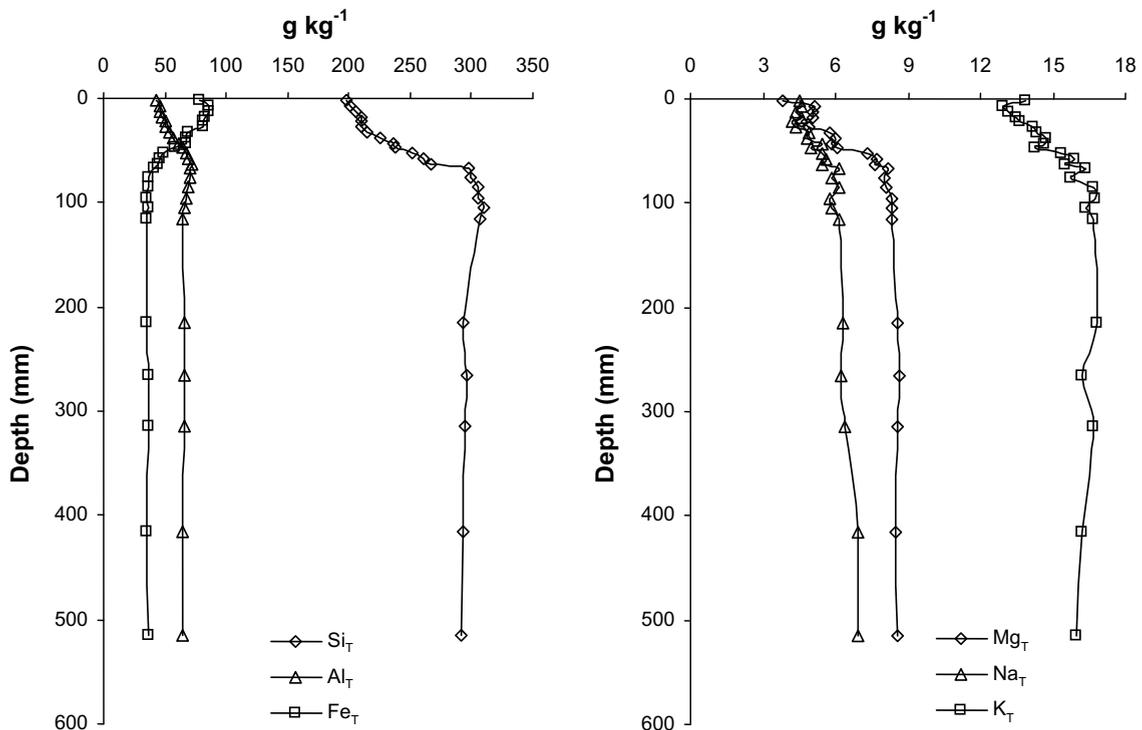
Fig. 2. Vertical distribution of total Si (Si_T), Al (Al_T), Fe (Fe_T), Mg (Mg_T), Na (Na_T) and K (K_T) in soil Q1.
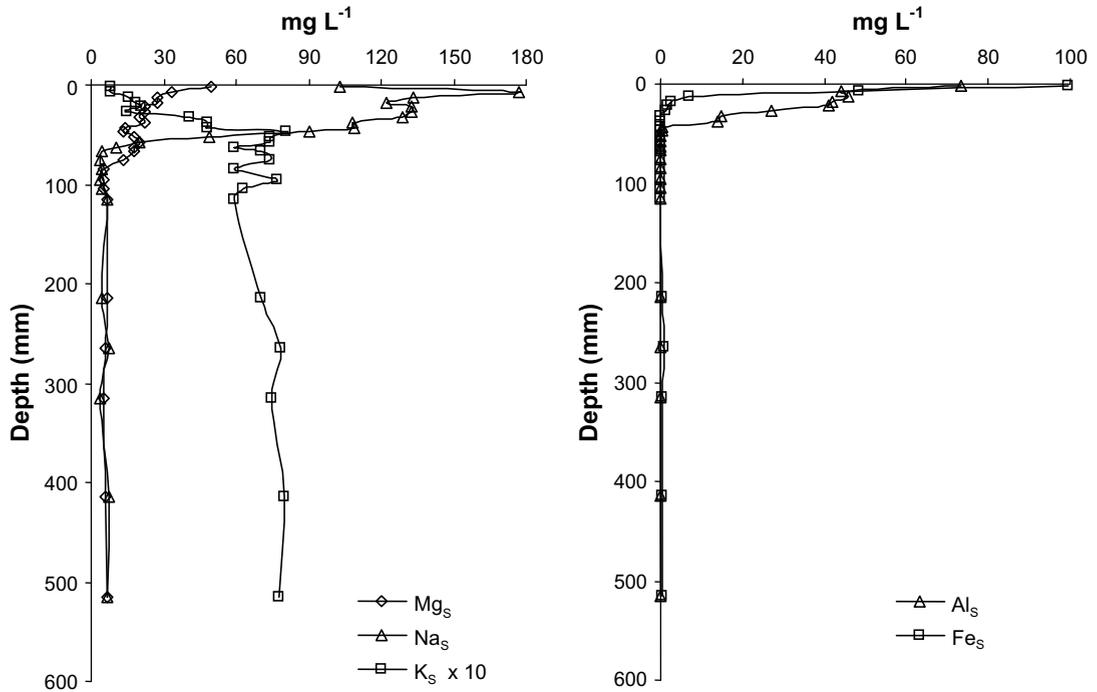
Fig. 3. Vertical distribution of water-soluble Al (Al$_s$), Fe (Fe$_s$), Mg (Mg$_s$), Na (Na$_s$) and K (K$_s$) in soil Q1.
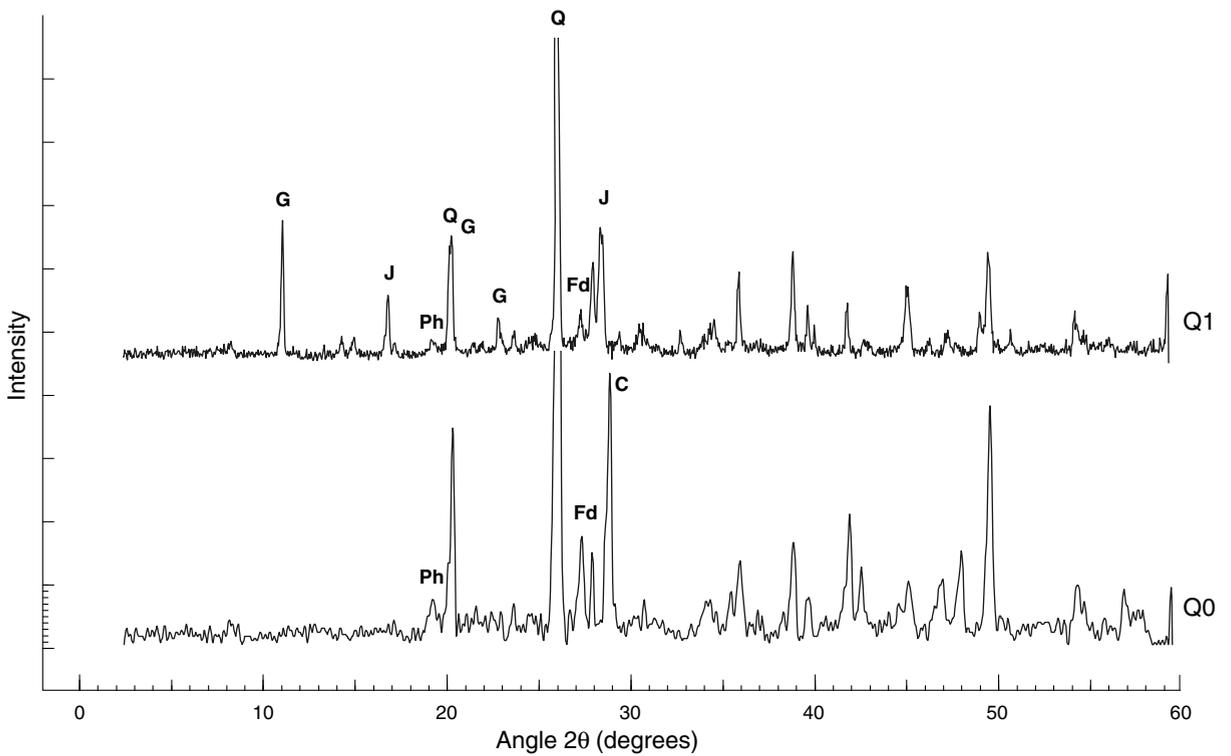
Fig. 4. X-ray diffractograms of soil Q0 and Q1 at 15–20 mm depth (C: calcite, Q: quartz, Fd: feldspars, Ph: phyllosilicates, G: gypsum, J: jarosite).

soil, while the other primary minerals showed major variations in abundance (Table 3). In this sense, the feldspars and phyllosilicates reduced significantly ($p < 0.01$) in the altered layer (0–70 mm) of the soil Q1, in relation to the unaffected part (Table 4).

The scanning electron microscope study revealed the general aspect of the reddish-brown layer of alteration of the Q1 soil (Fig. 5). This figure shows that the alteration of the phyllosilicates caused the opening of the mineral layers. Some feldspars were also altered, releasing their basic constituents (Si, Al, K) and precipitating with those from the acidic solution (Fe, S) in amorphous masses that filled the hollows from the dissolution of the minerals and cemented the ground mass of the soil. Additionally, the precipitation of neoformational minerals (gypsum and minerals of the jarosite group), as well as the amorphous ferruginous, aluminous and siliceous masses, surrounded many mineral grains and cemented the soil matrix.

Near the tailings layer, the continued action of the acidic solution from the oxidation of the tailings had provoked an intense leaching of the Fe of the

Table 3
Mineralogy of soil Q1 (values in %)

Depth	Q	C	Fd	Phy	G	J
0–5	*53*	*–*	*10*	*3*	*14*	*20*
5–10	**54**	**–**	**12**	**5**	**13**	**16**
10–15	**46**	**–**	**11**	**6**	**23**	**14**
15–20	**53**	**–**	**11**	**8**	**24**	**4**
20–25	**55**	**–**	**12**	**7**	**22**	**4**
25–30	**58**	**–**	**14**	**7**	**18**	**3**
30–35	**56**	**–**	**13**	**8**	**19**	**4**
35–40	**54**	**1**	**14**	**8**	**19**	**2**
40–45	**56**	**2**	**12**	**9**	**19**	**2**
45–50	**59**	**2**	**12**	**10**	**16**	**1**
50–55	**62**	**3**	**11**	**9**	**15**	**–**
55–60	66	**4**	**10**	**10**	**10**	**–**
60–65	64	**7**	**12**	**11**	**6**	**–**
65–70	62	**10**	**12**	**14**	**2**	**–**
70–80	65	9	14	12	–	–
80–90	66	10	13	11	–	–
90–100	62	12	14	12	–	–
100–110	65	11	12	12	–	–
110–120	61	10	15	14	–	–
190–240	59	12	16	13	–	–
240–290	61	11	13	15	–	–
290–390	60	12	15	13	–	–
390–490	62	11	14	13	–	–
490–590	59	10	17	14	–	–

Italics: light-grey layer; bold: reddish-brown layer; Q: quartz; C: calcite; Fd: feldspars; Phy: phyllosilicates; G: Gypsum; J: Jarosite-type minerals.

Table 4
Significant differences in feldspars and phyllosilicates in the affected (0–70 mm) and unaffected (>70 mm) soil samples

Mineral	Soil samples	Mean	S.D.	*p* value
Feldspars	Affected (0–70 mm)	11.9	1.2	<0.01
	Unaffected (>70 mm)	14.3	1.5	
Phyllosilicates	Affected (0–70 mm)	8.2	2.7	<0.01
	Unaffected (>70 mm)	12.9	1.2	

Values in %.

uppermost 5 mm of the profile, causing a relative impoverishment in this element, as reflected in Fig. 2. In the upper part of the reddish-brown layer (first 30 mm), the molar ratio of Fe:S was 1.3, very close to that of the minerals of the jarosite group [$KFe_3(SO_4)_2(OH)_6$], and the presence of these minerals was notable in the SEM study and in the mineralogical analysis by XRD. In this sense, deeper in the reddish-brown layer (30–45 mm), the Fe:S molar ratio rose to values higher than 2.3, indicating the presence of minerals with higher Fe contents than in jarosite (Fig. 6). Furthermore, the neoformation of schwertmannite-type minerals [$Fe_8O_8(OH)_6SO_4$] has been described in these media (Sánchez et al., 2005; Acero et al., 2006), and thus the presumed presence of this mineral may have contributed to the higher Fe:S molar ratio in this part of the profile. Finally, in the bottom part of the affected layer (45–70 mm), Fe oxyhydroxides with different degrees of crystallinity were detected in the SEM-EDX study.

4. Discussion

4.1. Soil properties and constituents

After 3 years of continued action of the acidic solution from the oxidation of the tailings, the soil properties and essential constituents had changed considerably, transforming the morphology and functionality of the original soil.

The decrease in pH is directly related to the intense acidification caused by the tailings oxidation and the infiltration into the soil of the acidic solution generated in this process. The EC of the soil solution registered the highest values in the uppermost 5 mm of the Q1 soil, implying an accumulation of soluble forms at this depth by the intense evapotranspiration in the area (Mediterranean climate); in this case, the soil solution was enriched in many elements, either directly from the oxidation of the
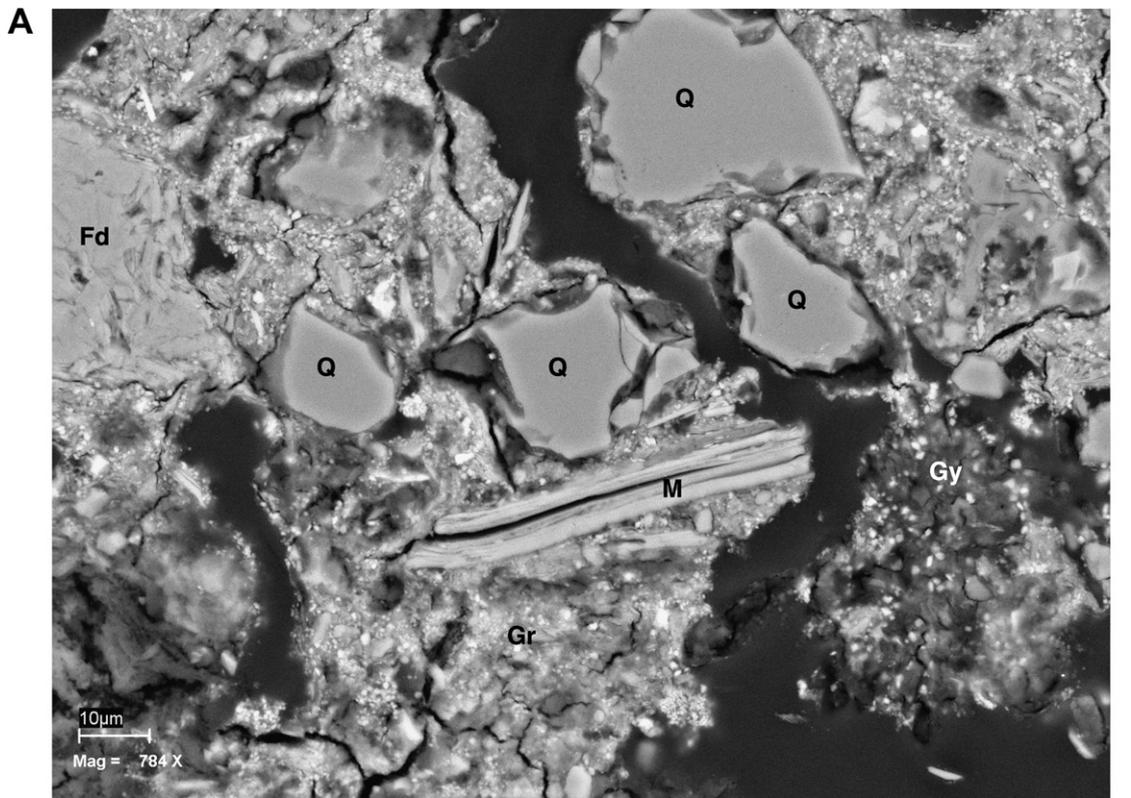
(Q: Quartz; M: Muscovite; Fd: Feldspars; Gy: Gypsum; Gr: Groundmass with microcrystals of jarosite)
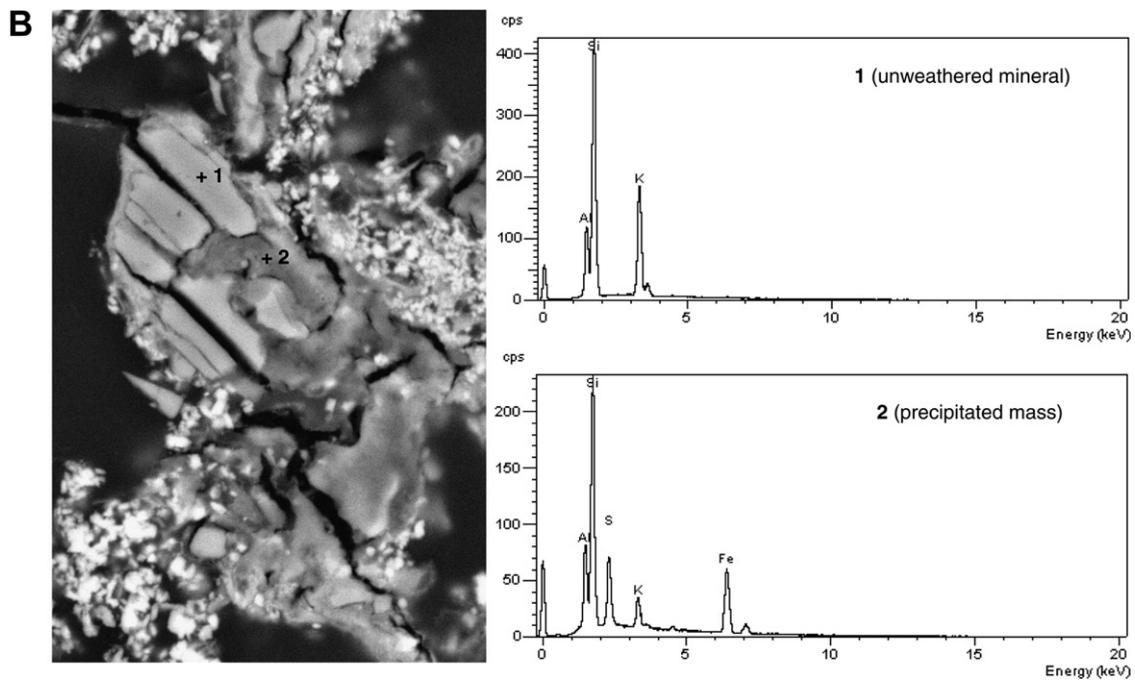
Fig. 5. SEM-BSE images of the mineral alteration in soil Q1. (A) General overview of the reddish-brown layer. (B) Alteration and EDX analysis of a feldspar.
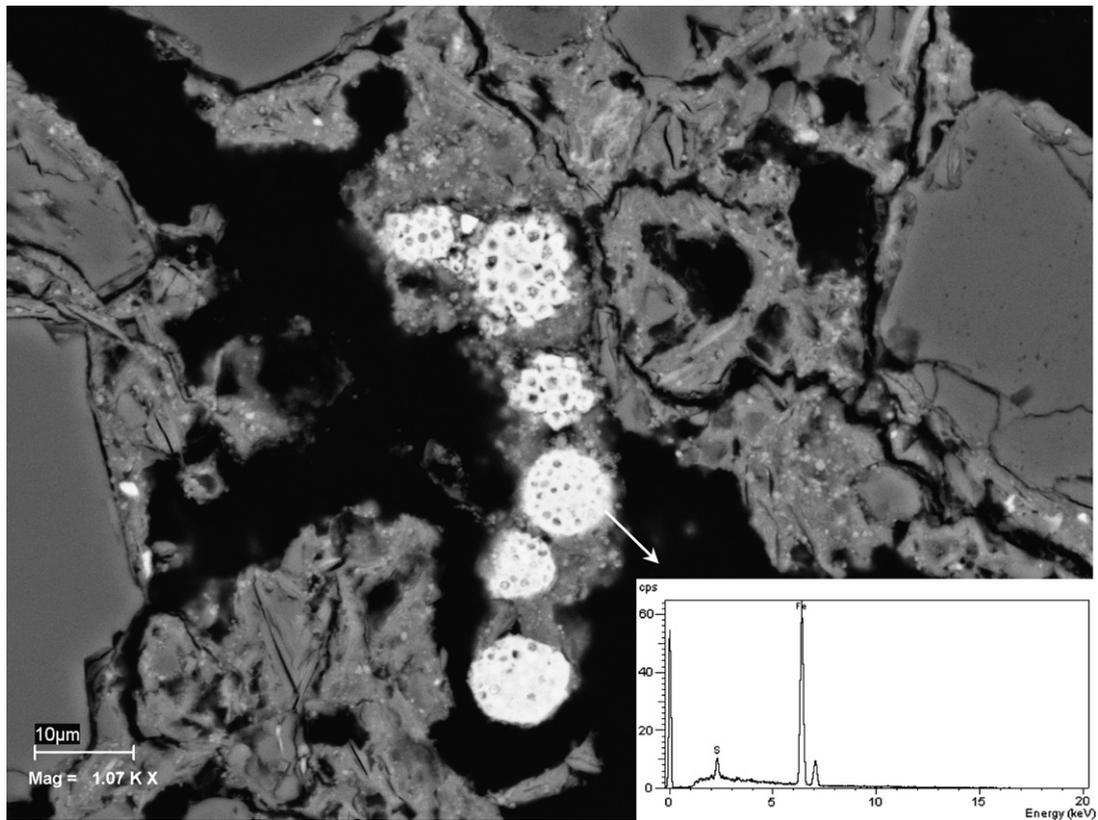
Fig. 6. SEM-BSE image and EDX analysis of Fe and S containing pedofeatures in soil Q1.

tailings or else from the alteration of the soil constituents. The regression analysis made between EC and the constituents present in the soil solution indicates that the increase in the values of this parameter was directly related to the concentration of SO_4^{2-} from the oxidation of sulphides present in the tailings, according to the following equation:

$$EC\ (dS\ m^{-1}) = 0.195 + 0.001SO_4^{2-}\ (mg\ l^{-1})\quad r^2$$
$$= 0.967;\quad p \leqslant 0.001$$

The clay content under these conditions is difficult to quantify, because the high concentrations of Fe from the oxidation of the tailings exert a powerful agglomerating effect on the smaller soil particles (Colombo and Torrent, 1991). This was clearly visible under the light microscope, revealing numerous aggregates of sand-grain sizes in which the clay had been bound by Fe compounds (Fig. 7). In this sense, a textural analysis was made of the Q1 samples, previously treated with dithionite–citrate–bicarbonate (DCB) to eliminate Fe oxides, and the results were compared with those of the same samples left untreated (Table 2). Thus, the

samples from the reddish-brown zone treated with DCB clearly increased in the quantity of clay present with respect to the untreated ones, reflecting the agglomerating power of the Fe oxides present.

The successive infiltrations into the soil of the acidic solutions from the oxidation of the tailings gave rise to the complete alteration of the carbonates in the first 35 mm of the Q1 soil and to its partial alteration between 35 and 80 mm. In this sense, a large part of the Ca^{2+} ions released in this weathering process of the carbonates reacted with the SO_4^{2-} ions of the acidic solution and precipitated in the form of gypsum (Ritsema and Groenenberg, 1993; Van Breemen, 1973), fundamentally in the first 80 mm of the soil (Table 3).

Also, in some zones the soil pH was below 6.5 and the $CaCO_3$ content was between 2 and 3% (Table 2, samples of 35–65 mm). This could be related to the coating of the coarse particles of these carbonates by the amorphous oxides and hydroxysulphates of Fe and Al, which protect against reactions with H^+ of the acidifying solution; this process has been previously observed in this soil (Simón et al., 2005).
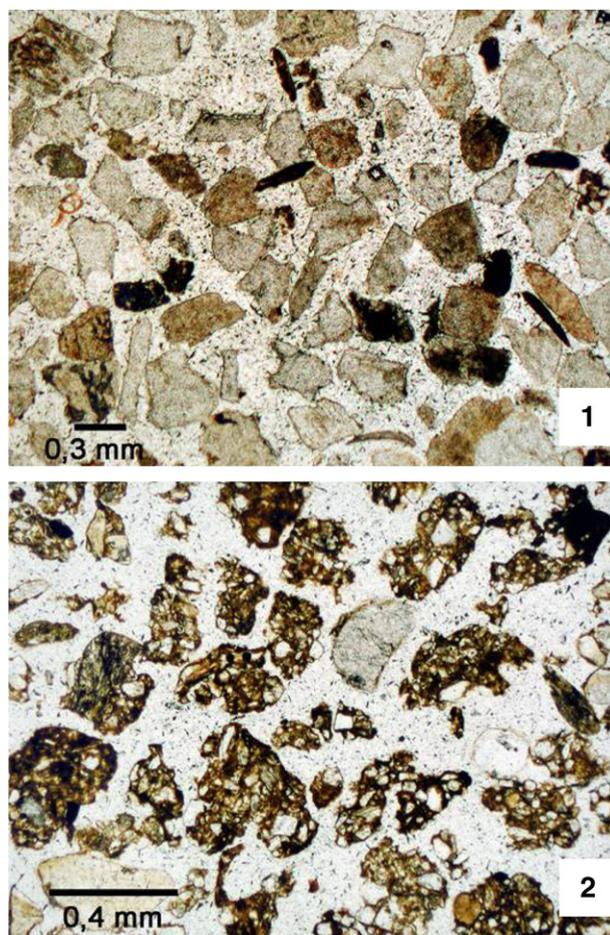
Fig. 7. Photomicrographs of coarse sands at 15–20 mm depth in soil Q0 (1) and at same depth in soil Q1 (2).

The total concentrations of the main elements (Si_T, Al_T, Mg_T, K_T, Na_T) clearly declined the first 70 mm of the Q1 soil and tended to increase with depth, confirming that the acidification partially altered the primary minerals such as feldspars and phyllosilicates (Preda and Cox, 2004).

The mobility of these elements appears to be closely related to soil pH. In this sense, Si_T and Al_T slightly differed, since the Al was leached in the strongly acidified zone and accumulated mainly from 55 to 95 mm in depth, where the pH was higher than 5.5, whereas the Si had greater relative mobility in these media, also leaching from the first cm of the soil but accumulating at a depth slightly greater than in the case of Al (70–120 mm in depth) and coinciding with the zone of pH > 7.5.

In the upper part of the soil, the Fe of the acidic solution coming from the oxidation of the tailings, entered the soil in the form of Fe^{2+}, but in the contact with this medium and after the pH rose above

2.3, it was oxidized to Fe^{3+} and subsequently precipitated.

The solubility of Fe and Al proved to be closely related to the pH of the soil. In the case of Fe, concentrations were very high in solution, the highest values reaching 0.1 g l^{-1} near the contact between the soil and the tailings, and maintaining high values to a depth of 15 mm, coinciding with a band of soil that had pH values lower than 2.3. Soluble Al also had very high concentrations in the upper part of the soil, reaching highs of 0.07 g l^{-1} in the contact zone between the soil and tailings, these high values persisting to a depth of 40 mm and coinciding with the band of soil with pH values lower than 5.5.

4.2. Mineralogical composition

The decline in soluble K could be related to the neoformation of jarosite in this zone of the soil (Dorronsoro et al., 2002; Simón et al., 2002;

Accornero et al., 2005). The variations commented on above were clearly visible as changes in the overall mineralogy of soil Q1 with depth. The large quantities of dissolved sulphates in the contaminant solution produced major mineralogical neoformations. Thus, on reacting with the Ca released in the alteration of the calcite, gypsum neoformation took place, this mineral reaching 20% of the total soil in some zones of the reddish-brown layer. On the other hand, the Fe and the total sulphates, together with the K released from the alteration of the feldspars and micas, formed jarosite-type Fe hydroxysulphates in large quantities (which reached 20% of the total mineralogy in some parts of the soil), coinciding with that of the most strongly acidified zone of the soil (Fukushi et al., 2003; Sánchez et al., 2005). In the uppermost part of the profile, the concentration of Pb reached $1.554.2\ \mathrm{mg\ kg^{-1}}$ (Martín et al., 2005), and the formation of plumbojarosite was expected, but its detection by X-ray diffraction was inconclusive, probably due to the low amount of this mineral in relation to the total mineralogy. The neoformation of this mineral, when the Pb concentration in soil is high, has been reported in sulphide oxidising solutions (Davis et al., 1999).

Most of the Fe released tended to precipitate in amorphous forms in the ground mass of the soil, being partially retained by neoformed minerals that became steadily more Fe enriched with depth down to 70–80 mm. As commented above, a large part of this Fe, after its subsequent oxidation, tended to precipitate as oxyhydroxysulphates, giving rise to a relationship between the total Fe and the SO_4^{2-} not precipitated as gypsum (S_{hs}), defined by the regression equation

$$S_{hs}\ (\mathrm{g\ kg^{-1}}) = -38.712 + 1.182\mathrm{Fe_T}(\mathrm{g\ kg^{-1}})$$
$$r^2 = 0.974; p \leqslant 0.001$$

In addition, the formation of jarosite was associated with the strongly acidic conditions of this part of the profile (Dold, 2003; Sánchez et al., 2005). Schwertmannite-type minerals and Fe oxyhydroxides, with low degrees of crystallinity and Fe contents far higher than the above-mentioned oxyhydroxysulphates, are common in these environments (Bigham et al., 1996; Sánchez et al., 2005). In the acidic media, schwertmannite can form, being capable of coexisting with jarosite under conditions of pH > 2.8 (Dold, 2003). Meanwhile, in neutral-alkaline environments, Fe oxyhydroxides such as ferrihydrite can form in the first stages (Davis

et al., 1999) and the transformation of this mineral to more stable Fe oxyhydroxides and oxides such as goethite and hematite has also been reported (Sun et al., 1996; Davis et al., 1999).

These mineralogical transformations and neoformations were of great importance in the study concerning the mobility and retention of the potentially contaminating elements involved, due primarily to the formation of minerals with a high specific surface area and a high degree of chemical reactivity (Carlson et al., 2002; Sastre et al., 2004). The changes in the properties and mineralogy of the soil due to the influence of pyrite oxidation, have important environmental implications and will influence the development of remedial measures to be applied to similar situations. These aspects will be examined in future studies.

5. Conclusions

The infiltration into the soil of the acidic solution from the oxidation of pyrite tailings is causing major morphological, compositional, and mineralogical changes in the profile of affected soils. After 3 years of continued action of such alteration, a considerable degradation of the main soil properties remains evident, the most notable being the decline in the cation-exchange capacity, texture variation, greater electrical conductivity (10-fold greater than in unaffected soil), and the appearance of horizons with colorations strongly differing from those of the original soil (a discoloured layer with greyish tonalities in the first 5 mm, followed by a reddish-brown layer to a depth of 65–70 mm). At the same time, the carbonates have weathered, disappearing completely from the first 35 mm and partially to 80 mm in depth. There was also an intense acidification of the soil (with pH values close to 2.0 within the greyish layer) as well as a partial hydrolysis of the primary silicates (mainly feldspars and phyllosilicates), provoking soil infertility.

The resulting products in this process give rise to intense neoformation of gypsum and hydroxysulphates (mainly jarosite), which, together with the acidic conditions of the medium, determine the mobility and distribution of the main elements of the soil, both in their total as well as soluble forms.

Acknowledgements

References

Accornero, M., Marini, L., Ottonello, G., Vetuschi, M., 2005. The fate of major constituents and chromium and other trace elements when acid waters from the derelict Libiola mine (Italy) are mixed with stream waters. Appl. Geochem. 20, 1368–1390.

Acero, P., Ayora, C., Torrentó, C., Nieto, J.M., 2006. The behavior of trace elements during schwertmannite precipitation and subsequent transformation into goethite and jarosite. Geochim. Cosmochim. Acta 70, 4130–4139.

Alastuey, A., García-Sánchez, A., López, F., Querol, X., 1999. Evolution of pyrite mud weathering and mobility of heavy metals in the Guadiamar valley after de Aznalcóllar spill, south-west Spain. Sci. Total Environ. 242, 41–55.

Bigham, J.M., Nordstrom, D.K., 2000. Iron and aluminum hydroxysulfates from acid sulfate waters. In: Alpers, C.N., Jambor, J.L., Nordstrom, D.K. (Eds.), Sulfate Minerals, vol. 40. Mineralogical Society of America, Reviews in Mineralogy and Geochemistry, pp. 351–403.

Bigham, J.M., Schwertmann, U., Traina, S.J., Winland, R.L., Wolf, M., 1996. Schwertmannite and the chemical modelling of iron in acid sulphate waters. Geochim. Cosmochim. Acta 60, 2111–2121.

Carlson, L., Bigham, J.M., Schwertmann, U., Kyek, A., Wagner, F., 2002. Scavenging of as from acid mine drainage by schwertmannite and ferrihydrite: a comparison with synthetic analogues. Environ. Sci. Technol. 36, 1712–1719.

Colombo, C., Torrent, J., 1991. Relationship between aggregation and iron oxides in Terra Rossa soils from Southern Italy. Catena 18, 51–59.

Davis, A., Eary, L.E., Helgen, S., 1999. Assessing the efficacy of lime amendment to geochemically stabilize mine tailings. Environ. Sci. Technol. 33, 2626–2632.

Dold, B., 2003. Dissolution kinetics of schwertmannite and ferrihydrite in oxidized mine samples and their detection by differential X-ray diffraction (DXRD). Appl. Geochem. 18, 1531–1540.

Dorronsoro, C., Martín, F., Ortíz, I., García, I., Simón, M., Fernández, E., Aguilar, J., Fernández, J., 2002. Migration of trace elements from pyrite tailings in carbonate soils. J. Environ. Qual. 31, 829–835.

FAO-ISRIC-ISSS, 1998. World Reference Base for Soil Resources. Roma.

Fukushi, K., Sasaki, M., Sato, T., Yanase, N., Amano, H., Ikeda, H., 2003. A natural attenuation of arsenic in drainage from an abandoned arsenic mine dump. Appl. Geochem. 18, 1267–1278.

Lacey, E.T., Lawson, F., 1979. Kinetics of the liquid-phase oxidation of acid ferrous sulfate by the bacterium Thiobacillus ferroxidans. Biotechnol. Bioeng. 12, 29–50.

López-Pamo, E., Barettino, D., Antón-Pacheco, C., Ortiz, G., Arránz, J.C., Gumiel, J.C., Martínez-Pledel, B., Aparicio, M., Montouto, O., 1999. The extent of the Aznalcóllar pyritic sludge spill and its effects on soils. Sci. Total Environ. 242, 57–88.

Loveland, P.J., Whalley, W.R., 1991. Particle size analysis. In: Smith, K.A., Mullis, C.E. (Eds.), Soil Analysis: Physical Methods. Marcel Dekker, New York, pp. 71–328.

Martín, F., Diez, M., García, I., Simón, M., Dorronsoro, C., Iriarte, A., Aguilar, J., 2005. Alteración de minerales primarios y movilidad de elementos mayoritarios en suelos afectados por un vertido de lodos piríticos. In: Jiménez, R., Álvarez, A.M. (Eds.), II Simposio nacional sobre control de la degradación de suelos. Madrid, Spain, pp. 533–537.

Nordstrom, D.K., 1982. Aqueous pyrite oxidation and the consequent formation of secondary iron minerals. In: Kitrick, J.A., Fanning, D.S., Hossner, L.R. (Eds.), Acid Sulfate Weathering, vol. 10. Soil Sci. Soc. Am. Madison, WI, pp. 37–56.

Norma DIN 38 414-4. German standard methods for the examination of water, waste water and sludge; determination of leachability by water (S 4). Deutsche Institut für Normung e.V. Berlín.

Palmer, M.E., 1978. Acidity and nutrient availability in colliery spoil. In: Goodman, G.T., Chadwick, M.J. (Eds.), Environmental Management of Minerals Wastes. Kluwer Academic Publishers..

Preda, M., Cox, M.E., 2004. Temporal variations of mineral character of acid-producing pyritic coastal sediments, Southeast Queensland, Australia. Sci. Total Environ. 326, 257–269.

Ritsema, C.J., Groenenberg, J.E., 1993. Pyrite oxidation, carbonate weathering, and gypsum formation in a drained potential acid sulfate soil. Soil Sci. Soc. Am. J. 57, 968–976.

Sánchez, J., López, E., Santofimia, E., Aduvire, O., Reyes, J., Barettino, D., 2005. Acid mine drainage in the Iberian Pyrite Belt (Odiel river watershed, Huelva, SW Spain): Geochemistry, mineralogy and environmental implications. Appl. Geochem. 20, 1320–1356.

Sastre, J., Hernández, E., Rodríguez, R., Alcobé, X., Vidal, M., Rauret, G., 2004. Use of sorption and extraction tests to predict the dynamics of the interaction of trace elements in agricultural soils contaminated by a mine tailing accident. Sci. Total Environ. 329, 261–281.

Sheldrick, B.H., Wang, C., 1993. Particle size distribution. In: Carter, M.R. (Ed.), Soil Sampling and Methods of Analysis. Canadian Society of Soil Science. Lewis Publishers, Boca Raton, Florida, pp. 99–511.

Simón, M., Dorronsoro, C., Ortiz, I., Martín, F., Aguilar, J., 2002. Pollution of carbonate soils in a Mediterranean climate due to a tailings spill. Eur. J. Soil Sci. 53, 1–10.

Simón, M., Martin, F., García, I., Bouza, P., Dorronsoro, C., Aguilar, J., 2005. Interactions of limestone grains and acidic solutions from the oxidation of pyrite taillings. Environ. Pollut. 135, 65–72.

Simón, M., Martín, F., Ortiz, I., García, I., Fernández, J., Fernández, E., Dorronsoro, C., Aguilar, J., 2001. Soil pollution by oxidation of tailings from toxic spill of a Pyrite mine. Sci. Total Environ. 279, 63–74.

Simón, M., Ortiz, I., García, I., Fernández, E., Fernández, J., Dorronsoro, C., Aguilar, J., 1999. Pollution of soils by the toxic spill of a pyrite mine (Aznalcóllar, Spain). Sci. Total Environ. 242, 105–115.

Stumm, W., Morgan, J.J., 1981. Aquatic Chemistry: An Introduction Emphasizing Chemical Equilibria in Natural Waters. John Wiley & Sons, New York.

Sun, T., Paige, C.R., Snodgrass, W.J., 1996. The effect of cadmium on the transformation of ferrihydrite into crystalline products at pH 8. Water Air Soil Pollut. 91, 307–325.

Van Breemen, N., 1973. Soil forming processes in acid sulfate soils. In: Dost, H. (Ed.), Acid sulfate Soils. Proc. Internat. Symp. 1st. ILRI Publ. 18. Inst. for Land Reclam. and Improve, vol. 2. Wageningen, The Netherlands, pp. 66–130.

Williams, D.E., 1948. A rapid manometric method for the determination of carbonate in soils. Soil Sci. Soc. Am. Proc. 13, 127–129.

Williams, E.G., Rose, A.W., Parizek, R.R., Waters, S.A., 1982. Factors controlling the generation of acid mine drainage. Final Rep. U.S. Bur. Mines. Res. Grant G5105086.